



# Long-term Impact of Carotid Endarterectomy on Choroidal and Choriocapillaris Perfusion: The INFLATE Study

Alessandro Berni, MD,<sup>1,2,\*</sup> Yi Zhang, PhD,<sup>3,\*</sup> Sandy Zhou Wenting, MD,<sup>1,4</sup> Natalie Noam, MD,<sup>5</sup> David Rabinovitch, BSc,<sup>6</sup> Basheer Sheick Yousif, MD,<sup>5</sup> Gissel Herrera, MD,<sup>1</sup> Mengxi Shen, MD, PhD,<sup>1</sup> Robert O'Brien, PhD,<sup>1</sup> Giovanni Gregori, PhD,<sup>1</sup> Ruikang K. Wang, PhD,<sup>3,7</sup> Philip J. Rosenfeld, MD, PhD,<sup>1</sup> Omer Trivizki, MD<sup>1,6</sup>

**Purpose:** When performed for clinically significant carotid artery stenosis (CAS), the long-term impact of carotid endarterectomy (CEA) on choroidal and choriocapillaris (CC) circulation was studied using swept-source OCT angiography.

**Design:** Prospective observational study.

**Participants:** Patients with clinically significant CAS undergoing unilateral CEA.

**Methods:** Swept-source OCT angiography scans were performed on both eyes at baseline (before CEA), within 1 week post-CEA (short-term follow-up [FU]), and  $\geq 30$  days post-CEA (long-term FU). Using validated algorithms, we measured mean choroidal thickness (MCT), choroidal vascularity index (CVI), choroidal vessel volume (CVV), CC flow deficit percentage (CC FD%), and CC thickness within the 5-mm circle centered on the fovea for both the eye ipsilateral to CEA (surgical side) and the contralateral eye (nonsurgical side). Multivariable regression analysis was conducted to evaluate the impact of baseline demographic and clinical factors on the changes in choroidal and CC parameters.

**Main Outcome Measures:** Both the short- and long-term changes in MCT, CVI, CVV, CC FD%, and CC thickness.

**Results:** The study included 58 eyes from 29 patients. Significant short-term improvements in MCT ( $P < 0.001$ ) and CC thickness ( $P = 0.006$ ) were observed post-CEA on the surgical side. Long-term FU showed sustained increases in MCT compared with baseline ( $P = 0.02$ ), while CC thickness was not significantly different from baseline ( $P = 0.10$ ). The CVI did not change significantly from baseline at either short-term ( $P = 0.45$ ) or long-term ( $P = 0.22$ ) FU on the surgical side. While CVV demonstrated a short-term rise immediately post-CEA ( $P < 0.001$ ), the difference was not statistically significant at the long-term evaluation ( $P = 0.06$ ). No significant improvement in CC FD% from baseline was observed at any visit post-CEA (short-term  $P = 0.81$ , long-term  $P = 0.91$ ). The nonsurgical side only showed a significant reduction in CVI at the long-term FU visit compared with before CEA ( $P = 0.01$ ). Clinical variables such as age, degree of stenosis, diabetes, hypertension, and smoking status did not greatly impact the outcomes.

**Conclusions:** Unilateral CEA demonstrated a sustained increase in MCT, suggesting persistent improvements in choroidal perfusion in the ipsilateral eye.

**Financial Disclosure(s):** Proprietary or commercial disclosure may be found in the Footnotes and Disclosures at the end of this article. *Ophthalmology Science* 2025;5:100651 © 2024 by the American Academy of Ophthalmology. This is an open access article under the CC BY-NC-ND license (<http://creativecommons.org/licenses/by-nc-nd/4.0/>).



Supplemental material available at [www.ophtalmologyscience.org](http://www.ophtalmologyscience.org).

Carotid artery stenosis (CAS) is characterized by the narrowing of the internal carotid artery (ICA) due to the development of atherosclerotic plaques.<sup>1</sup> Carotid artery stenosis represents a critical health concern due to its direct correlation to ischemic stroke, the third leading cause of death and disability combined worldwide.<sup>2</sup> The

consequences of CAS can extend beyond the brain, with the reduction of blood flow in the ophthalmic artery (OA), the ICA's first intradural branch.<sup>3–6</sup> Given the OA's central role in ocular circulation, clinically significant CAS can precipitate ocular symptoms and signs on the ipsilateral side of the affected artery, such as amaurosis fugax or ocular

ischemic syndrome, potentially heralding severe cerebral consequences.<sup>3,4,6</sup> Advanced diagnostic methods, including Doppler ultrasound and 4-dimensional flow magnetic resonance imaging, have shown decreased, absent, or even reversed blood flow in the OA among patients with severe CAS, underscoring the profound impact of CAS on the ocular circulation.<sup>5,6</sup>

Carotid endarterectomy (CEA) is one of the first-line treatments for stroke prevention in patients with clinically significant CAS.<sup>7</sup> In addition, several studies demonstrated that CEA restores blood flow in the OA, corrects reversed flow, and ameliorates ischemic ophthalmic symptoms.<sup>4,6,8,9</sup> Despite the potential therapeutic benefits of CEA to improve OA blood flow, the modalities traditionally employed to assess changes in ocular blood flow after CEA directly, such as Doppler ultrasound and 4-dimensional flow magnetic resonance imaging, face practical limitations in ophthalmology clinics due to their limited availability and the need for specialized operators. OCT is a convenient, widely available, and easily performed imaging method for the indirect measurement of OA perfusion.

Given these considerations, we previously reported on the use of swept-source OCT angiography (SS-OCTA) to explore ocular perfusion changes in patients undergoing CEA.<sup>10–12</sup> Swept-source OCT angiography imaging using a single dense raster macular scan can generate a volumetric 3-dimensional assessment of the choroidal and choriocapillaris (CC) perfusion. Since around 85% of the blood flow coming from the OA is directed toward the posterior ciliary arteries, which then directly supply the choroidal circulation, SS-OCTA provides a fast, noninvasive, and easily reproduced imaging modality to assess the vascular impact of CEA on the eye.<sup>13</sup>

Our initial report described patients with clinically significant CAS undergoing unilateral CEA, measuring changes in mean choroidal thickness (MCT) and the choroidal vascularity index (CVI) before and within 1 week after CEA.<sup>12</sup> The study observed significant choroidal thinning before surgery on the ipsilateral side of the CEA compared with the contralateral side. After surgery, a significant increase in the MCT was observed on the ipsilateral side, with no changes observed on the contralateral side. No significant alterations in the CVI were observed on both sides, highlighting the independence of the CVI measurements from the choroidal thickness (CT) measurements as previously described.<sup>14</sup> These results suggested a prompt and substantial improvement in ocular vascular perfusion shortly after CEA.

Building on this initial report, our subsequent research focused on the microvascular changes in the CC by assessing the impact of CEA on CC thickness and the percentage of CC flow deficits (CC FDs%).<sup>12</sup> At baseline, we found a significantly higher CC FD% in the eyes located on the surgical side compared with eyes on the nonsurgical side. After CEA, results showed a notable decrease in CC FD% and an increase in CC thickness within eyes on the surgical side, which suggested a beneficial impact from CEA on the microvascular perfusion of the CC. Our findings also showed an

immediate and significant positive impact of CEA on the circulation in the ipsilateral eye.

This present paper extends the findings from our previous reports and explores the long-term outcomes after CEA on both the choroidal and CC circulation and whether the short-term postsurgical improvements are sustained over time. In this extended longitudinal study, we report that the increase in MCT after CEA persisted over time while the CC measurements reverted back to baseline values.

## Methods

This prospective OCT imaging study was approved by the ethics committee of the Tel Aviv Medical Center at the University of Tel Aviv in Israel. Informed consent was obtained from each subject. This study was performed following the tenets of the Declaration of Helsinki and complied with the Health Insurance Portability and Accountability Act of 1996.

## Participants

Patients diagnosed with unilateral CAS and scheduled to undergo CEA between January 2021 and December 2022 were identified from the vascular surgery clinic at Tel Aviv Medical Center. Stenosis in the ICA was diagnosed by ultrasound and classified according to the North American Symptomatic Carotid Endarterectomy Trial criteria, with stenosis categorized as low (0%–40%), moderate (50%–60%), and severe (>70%). Clinically significant CAS was defined as stenosis >50%.<sup>15,16</sup> The decision for CEA was guided by the 2021 Society for Vascular Surgery guidelines for managing extracranial cerebrovascular disease.<sup>10</sup>

## Patient Data Collection

The patient's gender, age, degree of stenosis, medical history, including diabetes and hypertension, and the status of smoking were recorded. The blood pressure was measured at baseline before the CEA when SS-OCTA imaging was performed. In this study, patients were excluded if they could not undergo ocular imaging or if the condition of their ocular media significantly affected the ability of OCT to capture clear retinal images. This included cases with poor image quality due to factors such as significant central corneal scarring, lens opacities affecting the visual axis, and posterior capsule opacification. Additionally, exclusion criteria included conditions that could impact choroidal or CC integrities and assessments, such as retinal vascular occlusions, diabetic retinopathy, age-related macular degeneration, polypoidal choroidal vasculopathy, geographic atrophy, central serous chorioretinopathy, choroiditis, vitreomacular changes like traction or an epiretinal membrane, and history of retinal detachment, severe ocular trauma, previous retinal laser therapy, any vitreoretinal surgery, high refractive error, and glaucoma.

## Imaging Protocol

Patients underwent imaging using SS-OCTA scans (PLEX Elite 9000; Carl Zeiss Meditec) on both eyes at 3 time

points: 1 to 2 days before surgery (baseline visit), within 1 week after surgery (short-term follow-up [FU] visit), and after  $\geq 30$  days after surgery (long-term FU visit). All imaging was performed during morning clinics to minimize diurnal variation effects.<sup>17</sup> The SS-OCTA instrument's specifications include a laser central wavelength of 1050 nm, a bandwidth of 100 nm, and a scanning rate of 100k Hz, providing an axial resolution of  $\sim 5 \mu\text{m}$  in tissue and a lateral resolution of  $\sim 20 \mu\text{m}$ . The OCTA  $6 \times 6 \text{ mm}$  scanning protocol centered on the fovea was employed for all participants. This scan pattern consists of 500 A-scans per B-scan with 2 repeated B-scans at the same B-scan position to generate the OCTA images using the published complex optical microangiography algorithm,<sup>18</sup> and 500 horizontal B-scans resulting in a  $12 \mu\text{m}$  uniform spacing between A-scans and B-scans. Each A-scan was sampled with 1536 pixels, giving each pixel an axial dimension of  $\sim 2 \mu\text{m}$ . Scans with signal strength  $< 7$  were excluded, and all OCTA scans were normalized to a signal strength score of 9 to minimize signal strength variations between scans.<sup>19</sup> The side ipsilateral to the CEA was referred to as the surgical side, whereas the side contralateral to the CEA is referred to as the nonsurgical side.

### Choroidal and CC Measurements

Swept-source OCT angiography scans acquired at the 3 different time points (baseline, short-term FU, and long-term FU visits) were used for both choroidal and CC measurements, including (1) MCT;<sup>14</sup> (2) CVI;<sup>14</sup> (3) choroidal vessel volume (CVV);<sup>14</sup> (4) CC FD%, which is defined as the percentage of pixels representing flow deficits relative to all the pixels within a given region;<sup>20–25</sup> and (5) CC thickness.<sup>26</sup>

The choroidal measurements were obtained using a previously validated automated algorithm that detects the boundaries of Bruch's membrane (BM) and choroidal-scleral interface.<sup>27</sup> Briefly, OCT signal attenuation was corrected to enhance the contrast of the choroidal vessels and the choroidal-scleral interface to improve the accuracy of choroidal layer segmentations.<sup>28</sup> A color-coded en face CT map was then created using the distance between BM and the choroidal-scleral interface. In addition, the choroidal vessels were segmented using Otsu's method on the attenuation-corrected image. The CVV was obtained by calculating the volume of the segmented vessels, while the CVI was calculated as the ratio between the CVV and the total volume of the choroid. The en face CVV and CVI maps were then generated by mapping CVV and CVI values for each A-line.<sup>14,27,29</sup> Finally, MCT, CVV, and CVI measurements were averaged within 5-mm circles centered on the fovea on both the surgical and nonsurgical sides for regional analysis.

The CC en face flow images were segmented using an inner boundary positioned  $4 \mu\text{m}$  beneath BM and an outer boundary positioned  $20 \mu\text{m}$  beneath BM according to published guidance.<sup>30</sup> The BM was first detected by an automated segmentation algorithm with manual corrections performed if needed. The retinal vessel projection artifacts were then removed using a validated

algorithm,<sup>19</sup> and a compensation strategy using the corresponding CC en face structural images was employed to compensate for signal loss in the CC en face flow images due to the overlying anatomy.<sup>24</sup> Choriocapillaris flow deficit binary maps were finally generated by the fuzzy C-means method using adaptive thresholds with a diameter of flow deficits  $< 24 \mu\text{m}$  being removed from the maps to reduce noise.<sup>20</sup> To calculate the CC thickness, the OCTA scans were first flattened at the retinal pigment epithelium centerline.<sup>27,31</sup> The A-scan signals were then normalized by local averaging, and the position of the OCTA CC flow peak along each A-scan was detected. Mean CC thickness was defined as the full width at half maximum of the CC flow peak.<sup>26</sup> Choriocapillaris flow deficits and CC thickness were finally analyzed in circles centered on the fovea with diameters of 5 mm within the  $6 \times 6$  scan pattern on both the surgical and nonsurgical sides.

### Statistical Analysis

Statistical analyses were conducted using SAS version 9.4 (SAS Institute) and R (version 4.3.2, R Foundation for Statistical Computing) software.<sup>32</sup> Normality was checked by normal quantile-quantile plots. Results were expressed as mean and standard deviation ( $\pm$ ) or mean and 95% confidence interval (CI), as applicable. Covariance pattern models with a compound symmetry correlation structure between fellow eyes and an unstructured correlation matrix for longitudinal correlation of visits were used to analyze the outcomes MCT, CVI, CVV, CC FD%, and CC thickness in the 5-mm circle.<sup>33</sup>

Multivariable longitudinal regression analysis was used to assess the impact of variables including age, mean arterial pressure, degree of stenosis, diabetes, hypertension, and status of smoking on the changes of MCT, CVV, CVI, CC FD%, and CC thickness. *P* values  $< 0.05$  were considered statistically significant.

### Results

A total of 60 patients were originally enrolled in the INFLATE study and underwent both baseline and short-term assessments. However, 31 patients declined to participate further in the study, resulting in their absence from the long-term FU evaluation. Therefore, the current study includes a final cohort of 29 patients (58 eyes) who completed evaluations at all 3 time points. The mean  $\pm$  standard deviation age of patients was  $72.6 \pm 7.7$  years, and 23 participants (79.3%) were men. Twelve patients (41.4%) had diabetes, 25 (86.2%) had hypertension, and 14 (48.3%) were smokers. The mean degree of stenosis at baseline was  $86.3\% \pm 8.9\%$  on the surgical side and  $34.91\% \pm 19.9\%$  on the nonsurgical side, *P*  $< 0.001$ . The mean short-term FU time was  $3.8 \pm 2.6$  days, while the long-term FU time was  $170.1 \pm 85.9$  days. The demographic, clinical, and baseline OCT angiography characteristics of patients are provided in Table 1.

Table 1. Baseline Features of Participants (N = 29 Subjects)

Age (y), Mean $\pm$ SD			72.6 $\pm$ 7.7
Male gender, n (%)			23 (79.3)
Diabetes, n (%)			12 (41.4)
Hypertension, n (%)			25 (86.2)
Smoking, n (%)			14 (48.3)
	Surgical	Nonsurgical	P Value
Stenosis degree (%), mean $\pm$ SD	86.3 $\pm$ 8.9	34.9 $\pm$ 19.9	<0.001
OCTA parameters			
MCT (mean [95% CI], $\mu$ m)	223.1 (198.1, 248.1)	237.4 (212.4, 262.4)	0.17
CVV (mean [95% CI], mm <sup>3</sup> )	3.64 (3.18, 4.11)	3.95 (3.48, 4.41)	0.19
CVI (mean [95% CI])	0.59 (0.58, 0.60)	0.60 (0.59, 0.61)	0.06
CC FD% (mean [95% CI])	10.7 (10.0, 11.4)	10.2 (9.5, 10.9)	0.21
CC thickness (mean [95% CI], $\mu$ m)	6.7 (6.3, 7.0)	6.9 (6.6, 7.2)	0.15

CC = choriocapillaris; CC FD% = choriocapillaris flow deficit; CI = confidence interval; CVI = choroidal vascularity index; CVV = choroidal vessels volume; MCT = mean choroidal thickness; OCTA = OCT angiography; SD = standard deviation.

## Choroidal Parameters

For the 29 patients included in this study, the baseline MCT within the 5 mm fovea-centered circle was 223.1  $\mu$ m (95% CI: 198.1, 248.1) on the surgical side and 237.4  $\mu$ m (95% CI: 212.4, 262.4) on the nonsurgical side, with no significant difference observed ( $P = 0.17$ ). Postsurgery, the MCT on the surgical side showed a significant increase, with a mean of 246.0  $\mu$ m (95% CI: 219.4, 272.6) at the short-term FU visit ( $P < 0.001$ ). At the long-term FU, the MCT remained significantly elevated at 235.6  $\mu$ m (95% CI: 210.3, 260.9) compared with baseline ( $P = 0.02$ ), yet it showed a significant decrease from the short-term FU measurement ( $P = 0.03$ ). Conversely, the nonsurgical side exhibited no significant changes in MCT across the FU with all  $P$  values  $>0.09$ : short-term FU (243.6  $\mu$ m, 95% CI: 217.1, 270.2) and long-term FU (245.9  $\mu$ m, 95% CI: 220.6, 271.2).

In evaluating CVV at baseline, the surgical side presented with a mean CVV of 3.64 mm<sup>3</sup> (95% CI: 3.18, 4.11), while the nonsurgical side had a slightly higher mean of 3.95 mm<sup>3</sup> (95% CI: 3.48, 4.41). However, this difference was not statistically significant ( $P = 0.19$ ). In the short-term FU, the surgical side showed a notable increase in CVV, reaching a mean of 3.98 mm<sup>3</sup> (95% CI: 3.49, 4.47), with this change being statistically significant compared with the baseline ( $P < 0.001$ ). The long-term FU further showed an increase to a mean of 4.28 mm<sup>3</sup> (95% CI: 3.55, 5.00). However, the change from the baseline was not significant ( $P = 0.06$ ), and there was no significant difference between the short-term and long-term FU ( $P = 0.36$ ). On the nonsurgical side, the short-term FU revealed a minimal increase in CVV to a mean of 4.05 mm<sup>3</sup> (95% CI: 3.56, 4.54), which was not statistically significant when compared with presurgery values ( $P = 0.14$ ). Similar results were obtained for the long-term FU, where the mean CVV was 4.07 mm<sup>3</sup> (95% CI: 3.34, 4.80), indicating no significant change from the baseline ( $P = 0.71$ ) or the short-term FU ( $P = 0.95$ ).

Regarding the CVI, no significant difference was noted between the 2 sides at baseline (0.59, [95% CI: 0.58, 0.60] on the surgical side and 0.60, [95% CI: 0.59, 0.61] on the

nonsurgical side,  $P = 0.06$ ). The CVI on the surgical side remained relatively stable over time showing no significant changes, measuring 0.59 (95% CI: 0.58, 0.60) at short-term FU and 0.58 (95% CI: 0.57, 0.59) at long-term FU ( $P$ : 0.45 and 0.22, short-term vs. baseline and long-term vs. baseline, respectively). In contrast, the nonsurgical side exhibited a statistically significant decrease in CVI at the long-term FU (0.58 [95% CI: 0.57, 0.59]) compared with both the baseline ( $P = 0.01$ ) and the short-term FU (0.59 [95% CI: 0.58, 0.61],  $P = 0.02$ ). Figure 1 and Table 2 show the longitudinal changes of choroidal parameters on the surgical and nonsurgical sides.

Figure 2 presents the case of a patient experiencing a notable increase in MCT from a baseline measurement of 261.4  $\mu$ m to 305.3  $\mu$ m 4 days post-CEA on the surgical side. By the long-term FU, 110 days after CEA, the MCT had slightly decreased to 301.5  $\mu$ m but remained significantly elevated compared with the baseline. Additionally, there was a marked increase in CVV on the surgical side, rising from 4.38 mm<sup>3</sup> at baseline to 5.35 mm<sup>3</sup> in the short-term FU and slightly decreasing to 5.18 mm<sup>3</sup> by the long-term assessment. The CVI increased from 0.60 at baseline to 0.62 shortly after surgery before settling at 0.61 at the long-term assessment. No visually significant changes are present on the nonsurgical side.

## CC Parameters

At baseline, the mean CC FD% was similar in the surgical (10.7% [95% CI: 10.0, 11.4]) and nonsurgical sides (10.2% [95% CI: 9.5, 10.9]), with no significant difference ( $P = 0.21$ ). Throughout the FU, the surgical side maintained this mean with no statistically significant changes at either short-term (10.7% [95% CI: 10.0, 11.3]) or long-term FU visits (10.7% [95% CI: 10.1, 11.4]). The nonsurgical side also showed a consistent mean CC FD% at the FU time points, with means of 10.4% at both short-term (95% CI: 9.8, 11.1) and long-term FU visits (95% CI: 9.7, 11.0).

Between the surgical and nonsurgical sides, the CC thickness at baseline was comparable,  $P = 0.15$ . For CC



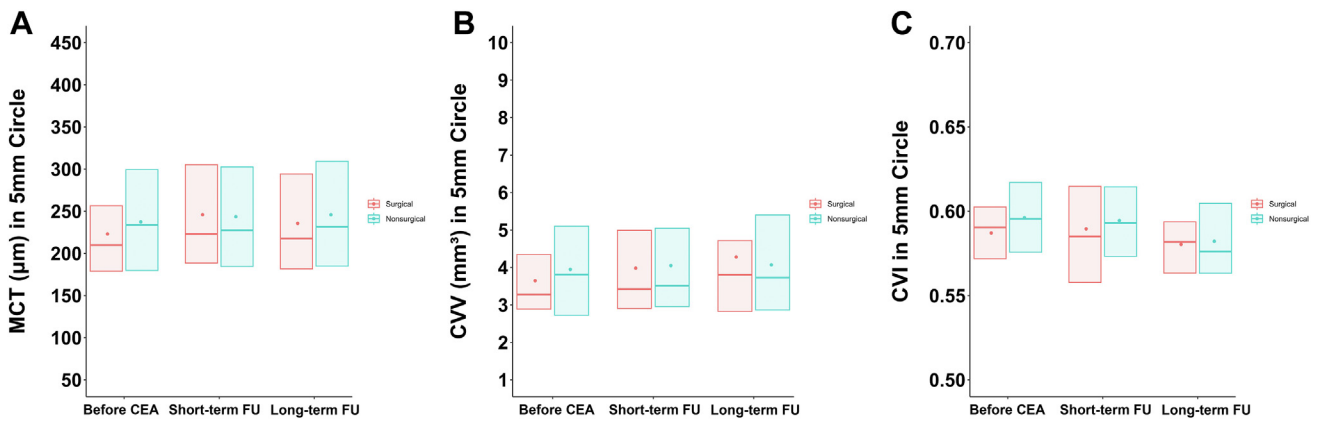


**Figure 1.** Box plots showing the distribution of MCT (A), CVV (B), and CVI (C) across 3 time points: before CEA, short-term FU, and long-term FU. Red boxes represent the surgical side, while blue boxes correspond to the nonsurgical side, with each measurement taken within a 5-mm circle centered on the fovea. The median value for each parameter is depicted by the central line of the box, and the mean is indicated by the dot. The extremities of the boxes define the first and third quartiles. CEA = carotid endarterectomy; CVI = choroidal vascularity index; CVV = choroidal vessel volume; FU = follow-up; MCT = mean choroidal thickness.

thickness on the surgical side, the baseline mean was 6.7  $\mu\text{m}$  (95% CI: 6.3, 7.0), with a statistically significant increase at the short-term FU to 7.0  $\mu\text{m}$  (95% CI: 6.6, 7.3,  $P = 0.006$ ). At the long-term FU, a slight reduction to 6.9  $\mu\text{m}$  (95% CI: 6.5, 7.2) was noted, with the changes from baseline ( $P = 0.10$ ), and short-term FU being nonsignificant ( $P = 0.45$ ). The nonsurgical side's mean CC thickness showed no significant changes, with measurements of 6.9  $\mu\text{m}$  (95% CI: 6.6, 7.2) at baseline, 7.0  $\mu\text{m}$  (95% CI: 6.6, 7.3) at the short-term FU, and 6.9  $\mu\text{m}$  (95% CI: 6.6, 7.2) long-term FU. Figure 3 and Table 3 present the longitudinal changes of CC parameters on the surgical and nonsurgical sides.

Figure 4 illustrates a case with one of the largest increases in CC thickness after CEA on the side ipsilateral to the surgery. Initially, the CC thickness was measured at 5.29  $\mu\text{m}$  at baseline, which then increased to 7.33  $\mu\text{m}$  4 days postsurgery. By the long-term FU, 235 days after CEA, the CC thickness had decreased to 5.71  $\mu\text{m}$  but was still higher than the initial baseline measurement. Additionally, the CC FD% on the surgical side showed a decrease from 14.3% at baseline to 12.2% in the short-term FU, with a small change to 12.43% in the long-term assessment.

### Multivariable Regression Analysis

We performed a multivariable longitudinal regression analysis to evaluate the effects of various factors, including FU duration (short- and long-term), age, presence of diabetes, hypertension, smoking status, and degree of stenosis on changes in choroidal and CC parameters postsurgery (Supplementary Tables 4–8, available at [www.ophtalmologyscience.org](http://www.ophtalmologyscience.org)). The only clinically relevant and statistically significant association in the multivariable models was a positive association between the degree of stenosis and changes in MCT from baseline on the surgical side ( $P = 0.02$ ).

### FU Loss Analysis

Given the significant number of patients lost to FU ( $N = 31$ , 51.7%), we analyzed baseline choroidal and CC parameters for all 60 patients initially enrolled in the study (Supplementary Table 9, available at [www.ophtalmologyscience.org](http://www.ophtalmologyscience.org)). Comparing the surgical and nonsurgical sides among these patients revealed that baseline MCT within the 5-mm circle was significantly lower on the surgical side ( $P = 0.007$ ), along with reduced CVV ( $P = 0.007$ ) and CVI ( $P = 0.015$ ). Additionally, the surgical side exhibited a thinner CC ( $P < 0.001$ ) and a higher CC FD% ( $P = 0.007$ ).

We also compared patients with long-term FU to those lost to FU across all demographic, clinical, and quantitative measures to identify any significant differences between the 2 groups (Supplementary Table 10, available at [www.ophtalmologyscience.org](http://www.ophtalmologyscience.org)). No significant differences were found between the cohorts for any variable except for hypertension status, with the long-term FU group having a higher percentage of patients with hypertension ( $P = 0.03$ ).

### Discussion

This study uses advanced SS-OCTA imaging techniques to provide a comprehensive analysis of the long-term changes in choroidal and CC circulation after CEA. Our observations extend and refine the results from our previously published short-term results, offering a deeper understanding of the ocular vascular changes post-CEA.<sup>11,12</sup> When analyzing the full dataset of 60 patients, we observed significant differences between the surgical and nonsurgical sides at baseline, aligning with our previous findings.<sup>11,12</sup> We had previously hypothesized that the reduced MCT on the stenotic side could be attributed to impaired circulation in the posterior ciliary

Table 2. Longitudinal Comparison of Choroidal Parameters on the Surgical and Nonsurgical Side (N = 29 Subjects)

Parameters	Baseline	Short-Term FU	Long-Term FU	P Value Baseline vs. Short-Term FU	P Value Baseline vs. Long-Term FU	P Value Short-Term FU vs. Long-Term FU
<b>Surgical side</b>						
MCT (mean [95% CI], $\mu\text{m}$ )	223.1 (198.1, 248.1)	246.0 (219.4, 272.6)	235.6 (210.3, 260.9)	<0.001	0.02	0.03
CVV (mean [95% CI], $\text{mm}^3$ )	3.64 (3.18, 4.11)	3.98 (3.49, 4.47)	4.28 (3.55, 5.00)	<0.001	0.06	0.36
CVI (mean [95% CI])	0.59 (0.58, 0.60)	0.59 (0.58, 0.60)	0.58 (0.57, 0.59)	0.45	0.22	0.07
<b>Nonsurgical Side</b>						
MCT (mean [95% CI], $\mu\text{m}$ )	237.4 (212.4, 262.4)	243.6 (217.1, 270.2)	245.9 (220.6, 271.2)	0.15	0.09	0.62
CVV (mean [95% CI], $\text{mm}^3$ )	3.95 (3.48, 4.41)	4.05 (3.56, 4.54)	4.07 (3.34, 4.80)	0.14	0.71	0.95
CVI (mean [95% CI])	0.60 (0.59, 0.61)	0.59 (0.58, 0.61)	0.58 (0.57, 0.59)	0.62	0.01	0.02

CEA = carotid endarterectomy; CI = confidence interval; CVI = choroidal vascularity index; CVV = choroidal vessels volume; FU = follow-up; MCT = mean choroidal thickness. Baseline: 1-2 days before CEA; short-term FU: 3.76  $\pm$  2.64 days after CEA; long-term FU: 170.07  $\pm$  85.89 days after CEA.

arteries, which receive reduced blood flow from the OA due to CAS.<sup>12</sup> The diminished blood flow in the eye on the stenotic side similarly explains the reduced CVV and CVI observed in these eyes.<sup>12</sup> Additionally, the reduced CC thickness and increased CC FD% on the surgical side corroborate our earlier results, further supporting the notion that CAS affects CC perfusion as well.<sup>11</sup> However, when focusing only on patients having long-term FU, these baseline choroidal and CC differences were no longer evident, likely due to the smaller sample size and probable selection bias. The comparison between patients lost to FU and those included in the long-term analysis showed no significant differences, indicating that the long-term patients can adequately represent the entire cohort. The only exception was a higher prevalence of hypertension in the long-term group. However, multivariable regression analysis did not identify any association between hypertension and changes in choroidal or CC parameters after surgery.

Despite the absence of baseline differences, the impact of CEA on the CT varied between the 2 sides within our long-term study population. After CEA, a significant elevation in MCT was detected only on the surgical side. Here, the MCT rose immediately after surgery and remained significantly higher at the long-term FU compared with baseline. This persistent increase underscores the durable positive impact of CEA on ocular vasculature, corroborating similar findings from other authors. For instance, the study by Lareyre et al<sup>34</sup> documented increases in MCT on the surgical side both at 1 month and 3 months postsurgery, and Krytowska et al,<sup>35</sup> while finding no immediate change in CT right after CEA, identified a significant increase 3 months later on the side ipsilateral to CEA. In contrast to our results, other studies relying on single B-scan measurements did not observe CT changes post-CEA, suggesting that CAS might not invariably impact the OA circulation. Specifically, Rabina et al<sup>36</sup> evaluated CT before and 14 months post-CEA in a small cohort of 8 patients and observed no significant alterations on the surgical side. They suggested that if preoperative CT is normal or comparable to the contralateral side, as seen in their study group, no significant changes should be expected post-CEA. Conversely, improvements would be anticipated only in eyes with significantly impaired CT at baseline due to reduced OA blood flow. However, even though in our long-term study population, there were no significant disparities between the ipsilateral and contralateral eyes, we still observed a post-CEA increase in MCT on the surgical side. Ala-Kauhalauma et al<sup>37</sup> also reported no improvements in CT 6 months after CEA and suggested that the ocular blood flow impairments induced by a severe degree of stenosis (>70%) might be irreversible and, hence, revascularization may not restore normal ocular circulation in these cases. Supporting this hypothesis, Akca Bayar et al<sup>38</sup> documented CT increase over time (at 1, 3, and 6 months postsurgery) exclusively in patients with <70% CAS. Our multivariable regression analysis instead identified a positive association between the degree of stenosis and the improvements in MCT, with significant increases in MCT observed despite the severe mean

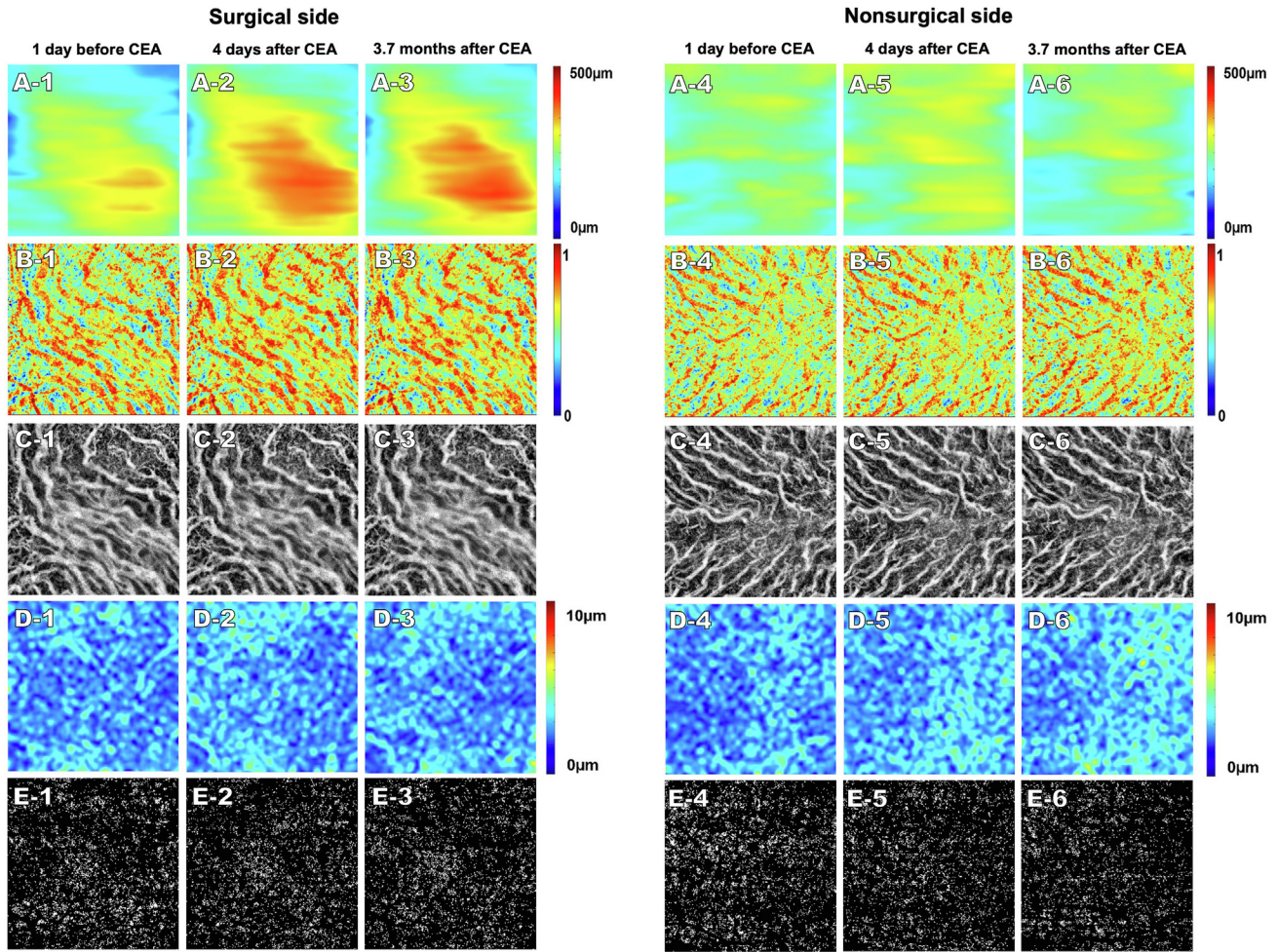


**Figure 2.** A 78-year-old patient with 80% CAS on the surgical side and 40% CAS on the nonsurgical side that underwent unilateral carotid endarterectomy (CEA) on the ipsilateral surgical side. Columns represent: (1&4) Baseline visit (3 days before CEA); (2&5) short-term FU visit (4 days after CEA); (3&6) long-term FU visit (3.7 months after CEA). Rows represent (A) choroidal thickness (CT) maps; (B) choroidal vascularity index maps; (C) en face choroidal vasculature map; (D) choriocapillaris (CC) thickness maps; (E) CC flow deficits binary maps. On the surgical side, there is a visually significant increase in both CT and CC thickness 4 days after CEA compared with 1 day before CEA (A-2 and D-2); the increase in CT was maintained in the long-term (A-3) while the CC thickness at the long-term visit was comparable to baseline (D-3). On the nonsurgical side, no visually significant changes at the long-term visit compared with before CEA were noted, except for a slight increase in CC thickness (D-6). CAS = carotid artery stenosis; FU = follow-up.

degree of stenosis (86%). Perhaps our volumetric approach to choroidal measurements and our measurements of MCT within the entire fovea-centered 5-mm circle provided a greater sensitivity, detecting changes that might have been missed by manual measurements on single B-scans. Another possible explanation for the absence of changes in MCT after revascularization procedures in some cases might be the presence of arterial stenosis in vessels located downstream of the ICA, possibly within the OA.<sup>39,40</sup>

A notable statistically significant increase in CVV was observed on the surgical side immediately after surgery, and the mean CVV remained elevated at the long-term FU, although statistical significance was not reached. While CEA should enhance blood flow in the OA, a direct correlation between improved OA circulation and

increased choroidal circulation has not been definitively established, even though systemic arterial vasodilators have been shown to increase choroidal perfusion, as demonstrated through swept-scan high-frequency digital ultrasound techniques.<sup>41,42</sup> However, the association between an increased carotid perfusion and an increase in choroidal perfusion assumes a normal OA without any stenoses.<sup>39,40</sup> If the perfusion of the OA increases after CEA, then we propose that the improved OA perfusion contributes to the elevated CVV detected on the surgical side post-CEA. The observed increase in CVV likely accounts for the higher MCT in our study. Future studies exploring the anatomy of the OA and whether stenoses are present might explain why some eyes had an increase in the MCT and CVV while other



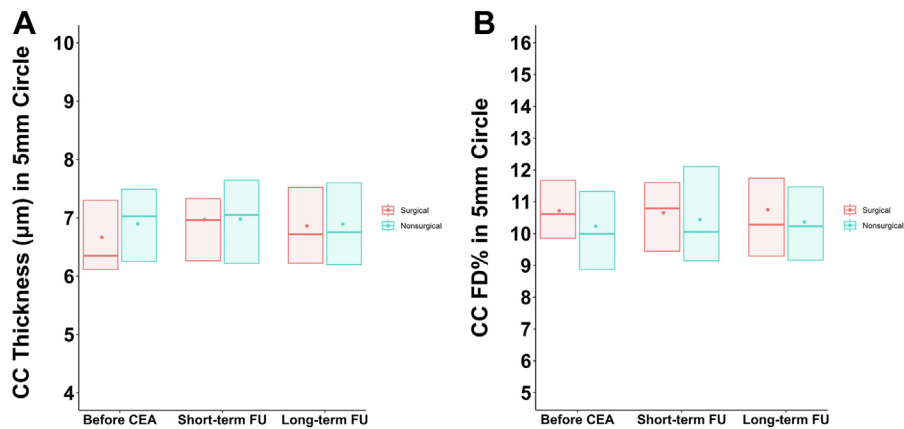


**Figure 3.** Box plots illustrating the distribution of CC thickness measurements (A) and CC FD% measurements (B) across 3 time points: before CEA, short-term FU, and long-term FU. The surgical side is indicated in red and the nonsurgical side in blue, and each parameter is measured within the 5-mm circle centered on the fovea. The central line of each box marks the median value of CC thickness or CC FD%, and the dot within indicates the mean. Box boundaries represent the first and third quartiles. CC = choriocapillaris; CC FD = choriocapillaris flow deficit; CEA = carotid endarterectomy; FU = follow-up.

eyes did not similarly respond to the CEA procedure. On the other hand, we were not surprised by the absence of significant variations in the CVI on the surgical side, either in the short or long term. The CVI reflects the ratio of CVV to the total choroidal volume, and since we observed an increase in both, there would not necessarily need to be a change in the CVI. We observed a similar situation in aging, where both the CT and CVV decreased, but not the CVI.<sup>14</sup>

After CEA, the acute increase in both the MCT and CVV on the surgical side was accompanied by a noticeable increase in CC thickness. At the long-term FU, the mean CC thickness remained high compared with baseline, but statistical significance was not reached, most likely due to the smaller number of patients analyzed. We did not find any changes in CC FD% compared with baseline in both short-term and long-term FUs on the side undergoing CEA.<sup>11</sup> The lack of longitudinal changes in CC FD% suggests that alterations in CC thickness, rather than FDs, could be more indicative of increased blood flow within the CC. This inference aligns with our prior observation of a mismatch between changes in CC FD% and CC thickness, where changes in volume appeared more pronounced than those related to flow.<sup>11</sup> We previously hypothesized that this divergence might stem from the methodological limitations of OCT angiography in measuring flow deficits, which are identified as areas of reduced or absent perfusion below the detection threshold of the device.<sup>11</sup> The process of binarizing OCT angiography images to calculate CC FD% might not fully capture actual improvements in blood flow, particularly in regions with initially low perfusion. Therefore, the observed increase in CC thickness might better represent the restoration of blood volume in these areas, which is not directly proportional to flow improvements. This would be consistent with a

situation where enhanced perfusion in capillaries might elevate thickness without necessarily altering flow deficit percentage. No existing research has explored the long-term changes in CC after CEA, underlining the unique value of our findings. Among the limited studies focusing on different CC parameters in CEA patients, none have found differences either before surgery or in short-term longitudinal FU visits post-CEA. In particular, Wan et al<sup>43</sup> analyzed the mean perfusion of the CC, defined as the length of microvessels in the perfused CC per unit area ( $\text{mm}^2$ ), whereas Pierro et al<sup>44</sup> employed a custom algorithm to evaluate the CC's vessel density, so their findings are not comparable with each other or with our study using CC FD% measurements.

Our study is marked by several strengths. First, the use of SS-OCTA allowed for deep choroidal penetration and reliable identification of choroidal structures. Second, unlike prior studies that depended on manual CT and CVI measurements from single B-scans,<sup>34–37,43,45</sup> we used validated semiautomated algorithms on dense SS-OCTA scans that allowed for measurements of MCT, CVI, and CC thickness in 3 dimensions. By measuring choroidal parameters within the fovea-centered 5-mm circle, we propose that our method ensures more accurate and reliable estimates of choroidal alterations than manual measurements from OCT B-scans. Third, while earlier attempts to study the CC involved methods like measuring CC microvessel length or CC vessel density, which are techniques limited by the insufficient resolution of current OCT devices to accurately identify CC capillaries, our study relied on an extensively validated methodology able to accurately quantify the extent of CC regions with reduced or absent perfusion (CC FDs).<sup>20–24,26</sup> The longitudinal nature of our research, building upon the patient population from previous reports, offers a unique perspective on the progression or stabilization of postsurgical vascular changes. This approach has not only



Table 3. Longitudinal Comparison of CC Parameters on the Surgical and Nonsurgical Side (N = 29 Subjects)

Parameters	Baseline	Short-Term FU	Long-Term FU	P Value Baseline vs. Short-Term FU	P Value Baseline vs. Long-Term FU	P Value Short-Term FU vs. Long-Term FU
<b>Surgical Side</b>						
CC FD% (mean [95% CI])	10.7 (10.0, 11.4)	10.7 (10.0, 11.3)	10.7 (10.1, 11.4)	0.81	0.91	0.65
CC thickness (mean [95% CI], $\mu\text{m}$ )	6.7 (6.3, 7.0)	7.0 (6.6, 7.3)	6.9 (6.5, 7.2)	0.006	0.10	0.45
<b>Nonsurgical Side</b>						
CC FD% (mean [95% CI])	10.2 (9.5, 10.9)	10.4 (9.8, 11.1)	10.4 (9.7, 11.0)	0.42	0.63	0.71
CC thickness (mean [95% CI], $\mu\text{m}$ )	6.9 (6.6, 7.2)	7.0 (6.6, 7.3)	6.9 (6.6, 7.2)	0.43	0.98	0.55

CEA = carotid endarterectomy; CC = choriocapillaris; CC FD% = choriocapillaris flow deficit; CI = confidence interval; FU = follow-up. Baseline: 1-2 days before CEA; short-term FU: 3.76  $\pm$  2.64 days after CEA; long-term FU: 170.07  $\pm$  85.89 days after CEA.

filled a gap in the current literature but also offered new insights into the discourse on the role of vascular surgery in enhancing choroidal perfusion. This will be particularly relevant in the context of conditions marked by reduced CC perfusion, such as diabetic retinopathy, central serous chorioretinopathy, and age-related macular degeneration, in which the restoration of blood flow in the OA is being investigated as a potential therapeutic avenue to improve choroidal blood flow.<sup>39,40</sup> Our research offered a strategy to study CC and choroidal parameters effectively, and our evidence can be used to better understand the impact of revascularization procedures both over the short- and long-term.

Despite these strengths, our study does have limitations. The long-term cohort size of this study was significantly smaller than the original number of patients included in the INFLATE study due to the challenges of scheduling long-term FU ophthalmic visits for vascular surgery patients. While assessments before and immediately after surgery were more easily performed, as these visits coincided with the patients' presurgical appointments or hospitalizations, it proved difficult to convince patients to return specifically for ophthalmic evaluations during the long-term FU period. This smaller size likely impacted the statistical significance of some changes in the long-term cohort compared with the short-term FU cohort. While the reasons for the loss of FU in these subjects were unlikely to selectively affect specific individuals, the possibility of selection bias cannot be completely ruled out. Secondly, in this study, we have decided to focus our analysis exclusively on the 5 mm fovea-centered circle, which is different from our earlier studies, where we also analyzed either the 2.5- or the 3-mm circles. This decision was guided by a strategic intent to streamline our investigation, aiming to balance the breadth of parameters examined without introducing an excessive number of variables that could potentially dilute the clarity of our findings. Nonetheless, the 5-mm circle covers a large area of the macula, providing a comprehensive view of the changes occurring in both the choroid and the CC. As stated in our previous publications,<sup>11,12</sup> the introduction of novel biomarkers for assessing the impact of CEA on ocular blood flow underscores the need for comparisons with established methods, such as OA Doppler ultrasound, a comparison that is currently limited by the technical challenges and routine clinical practices. Moreover, while our use of MCT, CVV, CVI, CCT, and CC FD % as surrogate markers offer valuable insights into choroidal and CC perfusion, a more comprehensive vascular assessment would necessitate direct measurement of blood flow within choroidal vessels, which is beyond the capabilities of our current technology. Finally, the lack of correlation with clinical visual function outcomes, such as visual acuity and microperimetry, limits our understanding of how these vascular changes translate into functional visual improvements.

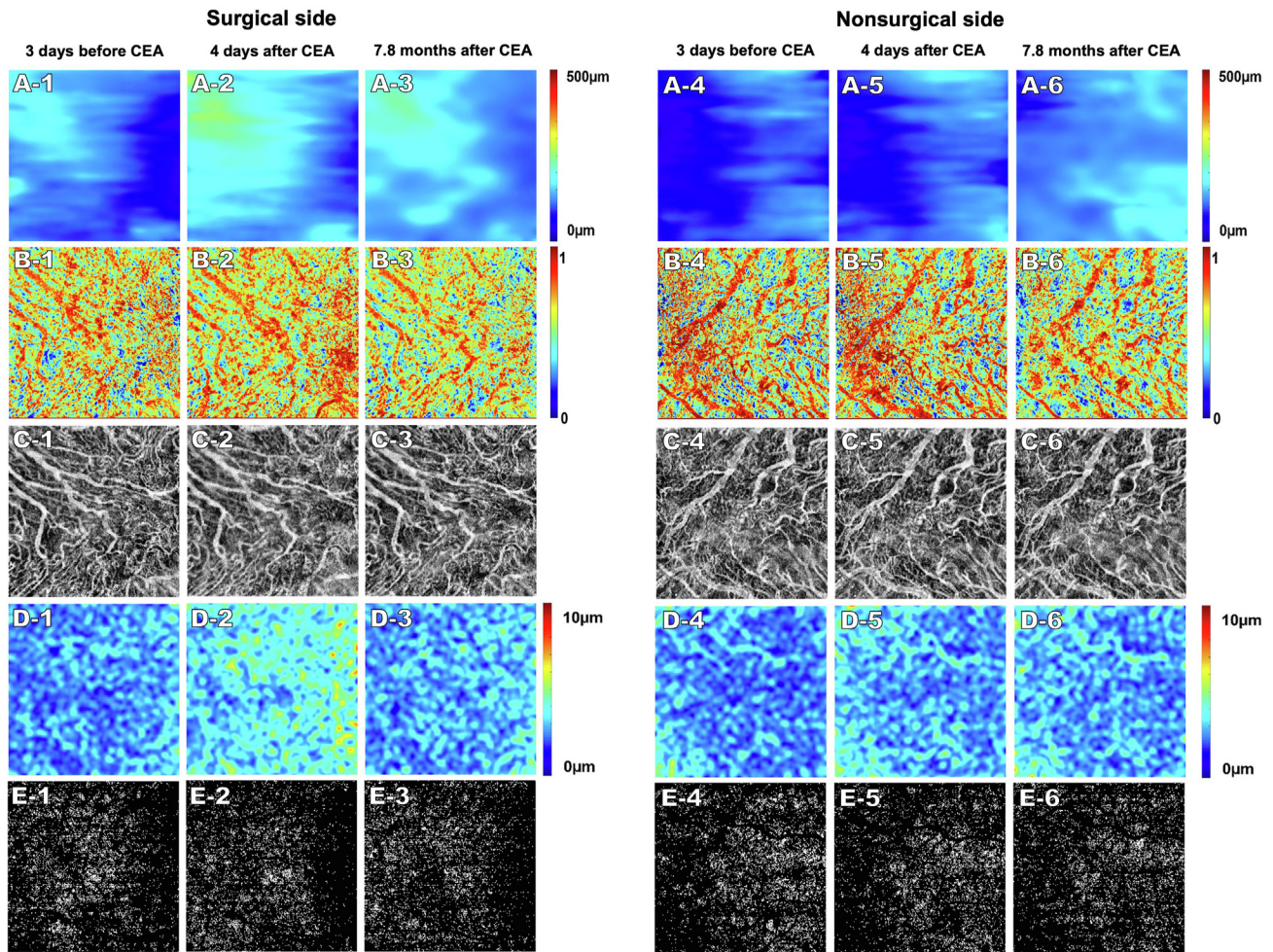


**Figure 4.** An 80-year-old patient with 95% CAS on the surgical side and 20% CAS on the nonsurgical side that underwent unilateral carotid endarterectomy (CEA) on the ipsilateral surgical side. Columns represent: (1&4) Baseline visit (3 days before CEA); (2&5) short-term FU visit (4 days after CEA); and (3&6) long-term FU visit (7.8 months after CEA). Rows represent (A) choroidal thickness (CT) maps; (B) choroidal vascularity index (CVI) maps; (C) en face choroidal vasculature map; (D) choriocapillaris (CC) thickness maps; (E) CC FDs binary maps. On the surgical side, there is a visually significant increase in CT 4 days after CEA compared with 3 days before CEA (A-1 vs. A-2); this increase was slightly reduced at the long-term assessment but was still increased compared with baseline (A-1 vs. A-3). There is an enlargement of choroidal vessels at the short-term FU visible both on the CVI maps (B-2) and on the en face choroidal vasculature maps (C-2). This increase was no longer evident at the long-term assessment (B-3 and C-3). There is also a visually significant increase in CC thickness at the short-term FU visit (D-2). The CC thickness returned to its baseline appearance at the long-term FU visit (D-3). No visually significant changes were noted in the CC FD maps (E-1, E-3). On the nonsurgical side, there was a subtle increase in the CT at the long-term assessment (A-6) compared with previous visits (A-4 and A-5), but no other significant changes at the long-term visit were appreciated when compared with baseline, 3 days before CEA (B-6, D-6). CAS = carotid artery stenosis; CC FD = choriocapillaris flow deficit; FU = follow-up.

In conclusion, by extending our previous short-term findings, we have offered deeper insights into the dynamics of ocular perfusion after CEA and captured the nuanced changes in the choroidal and CC circulation over time. Our findings highlight the persistence of increased CT on the eye ipsilateral to CEA and the stability of the CVI despite these changes. Our results clearly indicate that successful unilateral CEA positively impacts long-term choroidal perfusion in the ipsilateral eye.

### Declaration of Generative AI and AI-Assisted Technologies in the Writing Process

During the preparation of this work, the authors used ChatGPT4 in order to improve the manuscript's language and readability. After using this tool, the authors reviewed and edited the content as needed and take full responsibility for the content of the publication.

## Footnotes and Disclosures

Originally received: June 25, 2024.

Final revision: September 29, 2024.

Accepted: November 1, 2024.

Available online: November 8, 2024. Manuscript no. XOPS-D-24-00209R1.

<sup>1</sup> Department of Ophthalmology, Bascom Palmer Eye Institute, University of Miami Miller School of Medicine, Miami, Florida.

<sup>2</sup> Department of Ophthalmology, IRCCS San Raffaele Scientific Institute, Milan, Italy.

<sup>3</sup> Department of Bioengineering, University of Washington, Seattle, Washington.

<sup>4</sup> Department of Ophthalmology, Tan Tock Seng Hospital, National Health Group Eye Institute, Singapore, Republic of Singapore.

<sup>5</sup> Department of Vascular Surgery, Tel Aviv Medical Center, University of Tel Aviv, Tel Aviv, Israel.

<sup>6</sup> Department of Ophthalmology, Tel Aviv Medical Center, University of Tel Aviv, Tel Aviv, Israel.

<sup>7</sup> Department of Ophthalmology, University of Washington, Seattle, Washington.

\*A.B and Y.Z. contributed equally to the work presented here and should therefore be regarded as equivalent first authors.

Poster presentation at the 2024 Annual Association for Research in Vision and Ophthalmology Meeting, Seattle, WA. May, 2024.

### Disclosures:

All authors have completed and submitted the ICMJE disclosures form.

The authors have made the following disclosures:

G.G.: Grants — Carl Zeiss Meditec, National Eye Institute Center Core Grant (P30EY014801), Research to Prevent Blindness (unrestricted grant).

R.K.W.: Grants — Carl Zeiss Meditec Inc, National Eye Institute, The Research to Prevent Blindness, Colgate Palmolive Company, Estee Lauder Inc.; Consultant — Carl Zeiss Meditec, Cyberdantics; Honoraria — Carl Zeiss Meditec; Intellectual property — Oregon Health and Science University and the University of Washington; Patents planned, issued, or pending — US8, 750, 586, US8, 180, 134, US9, 282, 905, US9, 759, 544, US10, 354, 378, US10, 529, 061.

P.J.R.: Research support — Carl Zeiss Meditec, Inc. (University of Miami co-own a patent that is licensed to Carl Zeiss Meditec, Inc.); Grants — Gyroscope Therapeutics, Stealth BioTherapeutic, Carl Zeiss Meditec Inc, National Eye Institute, The Research to Prevent Blindness; Consultant — Abbvie, Annexon, Apellis, Bayer Pharmaceuticals, Boehringer-Ingelheim,

Carl Zeiss Meditec, Chengdu Kanghong Biotech, Genentech/Roche, InflammX Therapeutics, Ocudyne, Regeneron Pharmaceuticals, and Unity Biotechnology; Shares — Apellis, InflammX, Ocudyne, and Valitor.

O.T.: Grants — Voyant; Consultant — Truemed (Apellis), Galimedix.

Supported by research funding from Gyroscope Therapeutics (P.J.R.) and research support from Carl Zeiss Meditec Inc, Colgate Palmolive Company, and Estee Lauder Inc. (R.K.W.).

**HUMAN SUBJECTS:** Human subjects were included in this study. This prospective OCT imaging study was approved by the ethics committee of the Tel Aviv Medical Center at the University of Tel Aviv in Israel. Informed consent was obtained from each subject. This study was performed following the tenets of the Declaration of Helsinki and complied with the Health Insurance Portability and Accountability Act of 1996.

No animal subjects were used in this study.

### Author Contributions:

Conception and design: Berni, Zhang, Wenting, Noam, Rabinovitch, Yousif, Herrera, Shen, Gregori, Wang, Rosenfeld, Trivizki

Data collection: Berni, Zhang, Wenting, Noam, Rabinovitch, Yousif, Trivizki

Analysis and interpretation: Berni, Zhang, Wenting, Herrera, Shen, O'Brien, Gregori, Wang, Rosenfeld, Trivizki

Obtained funding: N/A

Overall responsibility: Berni, Zhang, O'Brien, Gregori, Wang, Rosenfeld, Trivizki

### Abbreviations and Acronyms:

**BM** = Bruch's membrane; **CAS** = carotid artery stenosis; **CC** = choriocapillaris; **CC FD%** = choriocapillaris flow deficit; **CEA** = carotid endarterectomy; **CI** = confidence interval; **CT** = choroidal thickness; **CVI** = choroidal vascularity index; **CVV** = choroidal vessel volume; **FU** = follow-up; **ICA** = internal carotid artery; **MCT** = mean choroidal thickness; **OA** = ophthalmic artery; **SS-OCTA** = swept-source OCT angiography.

### Keywords:

Carotid artery endarterectomy (CEA), Choriocapillaris flow deficits (CC FD), Choriocapillaris thickness, Choroidal vascular index (CVI), Mean choroidal thickness (MCT).

### Correspondence:

Omer Trivizki, MD, Department of Ophthalmology, Tel Aviv Medical Center, Waizman 6, Tel Aviv 6423906, Israel. E-mail: [omertr@gmail.com](mailto:omertr@gmail.com).

## References

- Qaja E, Tadi P, Theetha Kariyanna P. *Carotid Artery Stenosis*. Treasure Island (FL): StatPearls; 2024.
- Collaborators GBDS. Global, regional, and national burden of stroke and its risk factors, 1990-2019: a systematic analysis for the Global Burden of Disease Study 2019. *Lancet Neurol*. 2021;20:795–820.
- Mendrinis E, Machinis TG, Pournaras CJ. Ocular ischemic syndrome. *Surv Ophthalmol*. 2010;55:2–34.
- Kawaguchi S, Iida J, Uchiyama Y. Ocular circulation and chronic ocular ischemic syndrome before and after carotid artery revascularization surgery. *J Ophthalmol*. 2012;2012:350475.
- Sekine T, Takagi R, Amano Y, et al. 4D flow MR imaging of ophthalmic artery flow in patients with internal carotid artery stenosis. *Magn Reson Med Sci*. 2018;17:13–20.
- Nana P, Spanos K, Antoniou G, et al. The effect of carotid revascularization on the ophthalmic artery flow: systematic review and meta-analysis. *Int Angiol*. 2021;40:23–28.
- Murad MH, Shahrour A, Shah ND, et al. A systematic review and meta-analysis of randomized trials of carotid endarterectomy vs stenting. *J Vasc Surg*. 2011;53:792–797.
- Fujioka S. Use of orbital color Doppler imaging for detecting internal carotid artery stenosis in patients with amaurosis fugax. *Jpn J Ophthalmol*. 2003;47:276–280.
- Emiroglu MY, Evlice M, Akcakoyun M, et al. Effects of obstructive carotid artery disease on ocular circulation and the safety of carotid artery stenting. *Heart Lung Circ*. 2017;26:1069–1078.
- AbuRahma AF, Avgerinos ED, Chang RW, et al. Society for Vascular Surgery clinical practice guidelines for management



- of extracranial cerebrovascular disease. *J Vasc Surg.* 2022;75: 4S–22S.
11. Zhou SW, Zhang Y, Noam N, et al. The impact of carotid endarterectomy on choriocapillaris perfusion. *Invest Ophthalmol Vis Sci.* 2023;64:42.
12. Zhang Y, Zhou SW, Noam N, et al. Influence of carotid endarterectomy on choroidal perfusion: the INFLATE study. *Ophthalmol Retina.* 2024;8:62–71.
13. Michalinos A, Zogana S, Kotsiomitis E, et al. Anatomy of the ophthalmic artery: a review concerning its modern surgical and clinical applications. *Anat Res Int.* 2015;2015:591961.
14. Zhou H, Dai Y, Shi Y, et al. Age-related changes in choroidal thickness and the volume of vessels and stroma using swept-source OCT and fully automated algorithms. *Ophthalmol Retina.* 2020;4:204–215.
15. Naylor AR, Rothwell PM, Bell PR. Overview of the principal results and secondary analyses from the European and North American randomised trials of endarterectomy for symptomatic carotid stenosis. *Eur J Vasc Endovasc Surg.* 2003;26:115–129.
16. Bonati LH, Jansen O, de Borst GJ, Brown MM. Management of atherosclerotic extracranial carotid artery stenosis. *Lancet Neurol.* 2022;21:273–283.
17. Tan CS, Ouyang Y, Ruiz H, Sadda SR. Diurnal variation of choroidal thickness in normal, healthy subjects measured by spectral domain optical coherence tomography. *Invest Ophthalmol Vis Sci.* 2012;53:261–266.
18. Chu Z, Chen CL, Zhang Q, et al. Complex signal-based optical coherence tomography angiography enables in vivo visualization of choriocapillaris in human choroid. *J Biomed Opt.* 2017;22:1–10.
19. Zhang Q, Zhang A, Lee CS, et al. Projection artifact removal improves visualization and quantitation of macular neovascularization imaged by optical coherence tomography angiography. *Ophthalmol Retina.* 2017;1:124–136.
20. Chu Z, Zhang Q, Zhou H, et al. Quantifying choriocapillaris flow deficits using global and localized thresholding methods: a correlation study. *Quant Imaging Med Surg.* 2018;8: 1102–1112.
21. Zhang Q, Shi Y, Zhou H, et al. Accurate estimation of choriocapillaris flow deficits beyond normal intercapillary spacing with swept source OCT angiography. *Quant Imaging Med Surg.* 2018;8:658–666.
22. Zhang Q, Zheng F, Motulsky EH, et al. A novel strategy for quantifying choriocapillaris flow voids using swept-source OCT angiography. *Invest Ophthalmol Vis Sci.* 2018;59:203–211.
23. Chu Z, Gregori G, Rosenfeld PJ, Wang RK. Quantification of choriocapillaris with optical coherence tomography angiography: a comparison study. *Am J Ophthalmol.* 2019;208: 111–123.
24. Shi Y, Chu Z, Wang L, et al. Validation of a compensation strategy used to detect choriocapillaris flow deficits under drusen with swept source OCT angiography. *Am J Ophthalmol.* 2020;220:115–127.
25. Shi Y, Zhang Q, Zheng F, et al. Correlations between different choriocapillaris flow deficit parameters in normal eyes using swept source OCT angiography. *Am J Ophthalmol.* 2020;209:18–26.
26. Zhou H, Dai Y, Gregori G, et al. Automated morphometric measurement of the retinal pigment epithelium complex and choriocapillaris using swept source OCT. *Biomed Opt Express.* 2020;11:1834–1850.
27. Zhou H, Chu Z, Zhang Q, et al. Attenuation correction assisted automatic segmentation for assessing choroidal thickness and vasculature with swept-source OCT. *Biomed Opt Express.* 2018;9:6067–6080.
28. Zhou H, Lu J, Chen K, et al. Mitigating the effects of choroidal hyper- and hypo-transmission defects on choroidal vascularity index assessments using optical coherence tomography. *Quant Imaging Med Surg.* 2022;12:2932–2946.
29. Lu J, Zhou H, Shi Y, et al. Interocular asymmetry of choroidal thickness and vascularity index measurements in normal eyes assessed by swept-source optical coherence tomography. *Quant Imaging Med Surg.* 2022;12:781–795.
30. Chu Z, Zhang Q, Gregori G, et al. Guidelines for imaging the choriocapillaris using OCT angiography. *Am J Ophthalmol.* 2021;222:92–101.
31. Lu CD, Lee B, Schottenhamml J, et al. Photoreceptor layer thickness changes during dark adaptation observed with ultrahigh-resolution optical coherence tomography. *Invest Ophthalmol Vis Sci.* 2017;58:4632–4643.
32. Team RCR. *A Language and Environment for Statistical Computing.* Vienna, Austria: R Foundation for Statistical Computing; 2024.
33. Ying GS, Maguire MG, Glynn RJ, Rosner B. Tutorial on biostatistics: longitudinal analysis of correlated continuous eye data. *Ophthalmic Epidemiol.* 2021;28:3–20.
34. Lareyre F, Nguyen E, Raffort J, et al. Changes in ocular subfoveal choroidal thickness after carotid endarterectomy using enhanced depth imaging optical coherence tomography: a pilot study. *Angiology.* 2018;69:574–581.
35. Krytkowska E, Masiuk M, Kawa MP, et al. Impact of carotid endarterectomy on choroidal thickness and volume in enhanced depth optical coherence tomography imaging. *J Ophthalmol.* 2020;2020:8326207.
36. Rabina G, Barequet D, Mimouni M, et al. Carotid artery endarterectomy effect on choroidal thickness: one-year follow-up. *J Ophthalmol.* 2018;2018:8324093.
37. Ala-Kauhaluoma M, Koskinen SM, Silvennoinen H, et al. Subfoveal choroidal thickness in ipsi- and contralateral eyes of patients with carotid stenosis before and after carotid endarterectomy: a prospective study. *Acta Ophthalmol.* 2021;99: 545–552.
38. Akca Bayar S, Kayaarasi Ozturker Z, Pinarci EY, et al. Structural analysis of the retina and choroid before and after carotid artery surgery. *Curr Eye Res.* 2020;45:496–503.
39. Lylyk I, Bleise C, Lylyk PN, et al. Ophthalmic artery angioplasty for age-related macular degeneration. *J Neurointerv Surg.* 2022;14:968–972.
40. Rosenfeld PJ, Trivizki O, Gregori G, Wang RK. An update on the hemodynamic model of age-related macular degeneration. *Am J Ophthalmol.* 2022;235:291–299.
41. Vance SK, Imamura Y, Freund KB. The effects of sildenafil citrate on choroidal thickness as determined by enhanced depth imaging optical coherence tomography. *Retina.* 2011;31:332–335.
42. Kim DY, Silverman RH, Chan RV, et al. Measurement of choroidal perfusion and thickness following systemic sildenafil (Viagra(R)). *Acta Ophthalmol.* 2013;91:183–188.
43. Wan J, Kwapong WR, Tao W, et al. Choroidal changes in carotid stenosis patients after stenting detected by swept-source optical coherence tomography angiography. *Curr Neurovasc Res.* 2022;19:100–107.
44. Pierro L, Arrigo A, De Crescenzo M, et al. Quantitative optical coherence tomography angiography detects retinal perfusion changes in carotid artery stenosis. *Front Neurosci.* 2021;15: 640666.
45. Biberoğlu E, Eraslan M, Midi I, et al. Ocular blood flow and choroidal thickness changes after carotid artery stenting. *Arq Bras Oftalmol.* 2020;83:417–423.